

Reprinted from

Seventh International Symposium

Machine Processing of

Remotely Sensed Data

with special emphasis on

Range, Forest and Wetlands Assessment

June 23 - 26, 1981

Proceedings

Purdue University
The Laboratory for Applications of Remote Sensing
West Lafayette, Indiana 47907 USA

Copyright © 1981

by Purdue Research Foundation, West Lafayette, Indiana 47907. All Rights Reserved.

This paper is provided for personal educational use only,
under permission from Purdue Research Foundation.

Purdue Research Foundation

COMPLETE LINEAMENT EXTRACTION WITH THE AID OF SHADOW-FREE LANDSAT IMAGE

KIYONARI FUKUE, HARUHISA SHIMODA,
TOSHIBUMI SAKATA

Tokai University
Kanagawa, Japan

I. ABSTRACT

LANDSAT images are most useful for geological lineament extraction, especially for large-scale lineaments. However, because of the nature of the LANDSAT orbit, there are almost no lineaments in the same direction as the sun angle. In this report, a new technique which can generate virtual LANDSAT images with any sun directions is described.

In order to eliminate shadows from the original LANDSAT image, a shadow-free land cover classification was first applied. Shadow areas were classified into four categories using spectral features. Pixel values in each category of the original image were scaled to the values of corresponding categories in no-shadow areas, by coinciding the mean and standard deviation of each spectral band.

Next, a three-dimensional model of the object area was constructed from the National Land Information Data Base. Assuming a specific sun elevation and azimuth, the shadowed areas can be calculated from this model.

A cosine correction was made using the angle between the sun light axis and the plane direction. In addition, reflective intensities were calculated according to a three-dimensional reflective model. An artificially shadowed LANDSAT image with specific sun angle was thus obtained.

For lineament extraction, a sun azimuth was selected perpendicular to the real sun azimuth. A complete set of lineaments was obtained by combining the two results extracted from these two images. Furthermore, the influence of sun elevation on lineament enhancements is also discussed.

In conclusion, a technique to generate a virtual LANDSAT image with illumination at any sun angle was established. With

the aid of this virtual image, lineament extraction becomes more complete.

II. INTRODUCTION

In the last decade, remote sensing technologies have been more and more utilized in geological investigations. One of the most important image processing in this area is a lineament enhancement or extraction. LANDSAT MSS images are useful in this application, especially for large area investigations.

However, there is one big disadvantage in LANDSAT MSS images of mountainous areas. Most of lineaments in mountainous areas are generated from the shadows of mountains. The direction of shadows in LANDSAT images are almost constant, because LANDSAT is a sun synchronous satellite.

Therefore, lineaments which are perpendicular to the sun direction are evident but those which are parallel are very difficult to appear.

In this report, a method to generate a virtual LANDSAT image in which the sun direction can be varied is described.

III. METHOD

Fig.1 shows a flow chart of generating a virtual LANDSAT MSS image. In order to make an image which are illuminated from an arbitrary sun angle, shadows in the original LANDSAT image should be eliminated. In this research, this process was done with the aid of a shadow free classification.

Fig.2 shows the original LANDSAT MSS image used in this research. This image was first classified into fifteen categories including shadow areas. These categories are shown in Table 1.

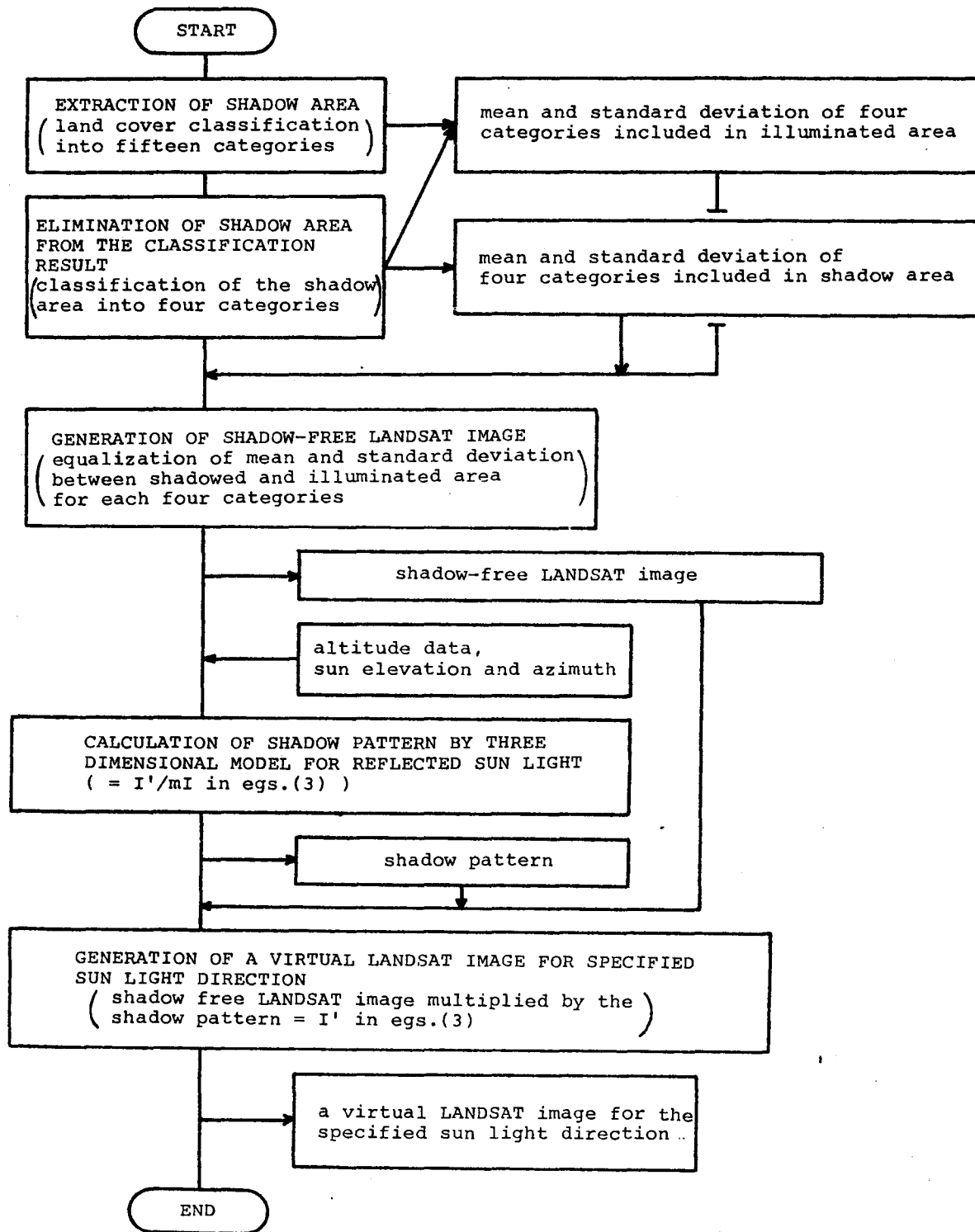


Fig.1 A flow chart of generating a virtual LANDSAT MSS image.

Table 1 Land Cover Classification Categories.

-
1. High Density Urban Areas
 2. Urban Areas
 3. Factories
 - * 4. Rice Fields and Grass Lands
 5. Crop Fields
 6. Golf Courses
 - * 7. Conifer Forests
 - * 8. Broad Leaved Forests
 - * 9. Mixed Forests
 10. Bare Grounds and Sands
 11. Water Bodies
 12. Snows
 13. Unclassified
 14. Lava
 - * 15. Shadows
-



Fig.2 The original LANDSAT image.

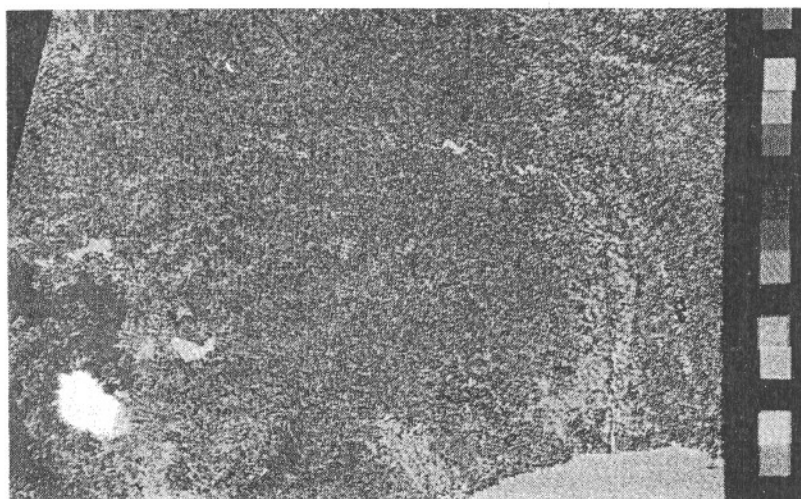


Fig.3 A classified result of LANDSAT image.

With the aid of ground truth data, these shadowed areas were found to be composed of four categories, i.e., conifer forests, broad leaved forests, mixed forests and grass lands. As the spectral differences were found according to these categories in the shadow areas, shadowed areas were further classified into these four categories using a maximum likelihood classification. Fig.3 shows the result.

According to the assumption that the same categories might have the same spectral features between the shadowed and illuminated regions, the means and standard deviations of the shadowed areas were coincided with those of the illuminated areas of corresponding categories. Fig.4 shows the resultant shadow free LANDSAT image.

The second task of this research is to make a three dimensional model of the test area. The necessary altitude data of the test area was given by the Land Numerical Information Data Base made by the Land Agency of Japan. The ground resolution of this altitude data is 2.25 minutes in longitude and latitude direction, respectively, while the LANDSAT data has a ground resolution of 0.45 minutes after the geometric correction and resampling.

The altitude data were interpolated in order to coincide its ground resolutions to that of LANDSAT data. A three dimensional model of LANDSAT data was thus acquired.

The last task is the shadow generation according to the three dimensional model. The details are given below.

IV. THREE DIMENSIONAL MODEL OF SHADOW GENERATIONS

Suppose the angle between the normal of the earth surface and the sun light axis to be θ_{sg} . Then the earth surface illuminance E is given as

$$E = (I/d) * \cos\theta \quad \dots\dots(1)$$

by cosine law. Here, "I" denotes the radiance of the sun light, "d" is the distance between the sun and the earth surface and θ_{sg} is the angle between the sun light axis and the normal of the earth surface.

The spatial distribution characteristics of reflected light can be approximated by

$$I' = a * \exp(-\theta_{rv}*b) * E \quad \dots\dots(2)$$



Fig. 4 A shadow free LANDSAT image.

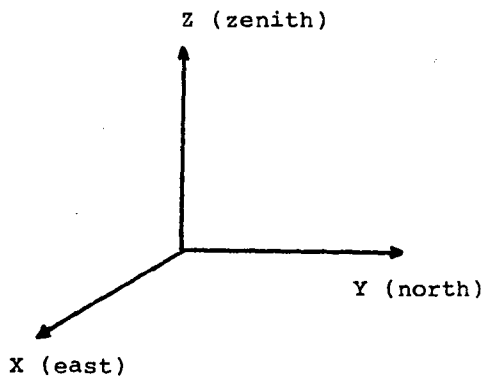


Fig.5 The X,Y,Z coordinate system.

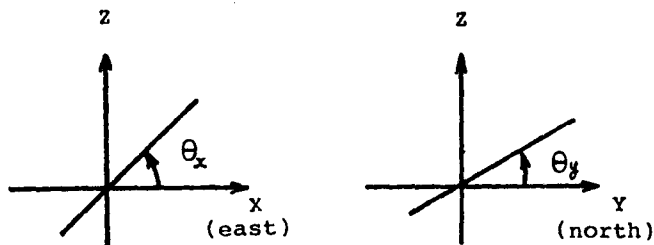


Fig.6 The slant angle θ_x and θ_y .

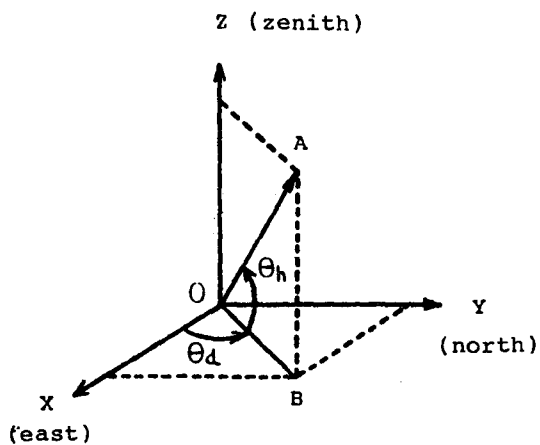


Fig.7 The sun elevation(θ_h) and azimuth(θ_d).

Here,
 θ_{rv} : angle between view direction and mirror reflection light axis.
 a, b : constant.

From the equations (1) and (2), the observed light strength of earth reflection I' from zenith can be expressed by

$$I' = mI \cdot \cos\theta_{sg} \cdot \exp(-\theta_{rv} \cdot n) \dots (3)$$

(m, n : constant)

Suppose the x, y, z coordinates as shown in Fig.5. By denoting the slant angle of the earth surface of x and y directions as θ_x and θ_y , respectively as shown in Fig.6 and the sun elevation and azimuth to be θ_h and θ_d , respectively (Fig.7), the direction cosines of the tangent plane of the earth G_x, G_y, G_z are expressed as

$$\begin{aligned} G_x &= \tan\theta_x / N \\ G_y &= \tan\theta_y / N \\ G_z &= 1 / N \end{aligned} \dots (4)$$

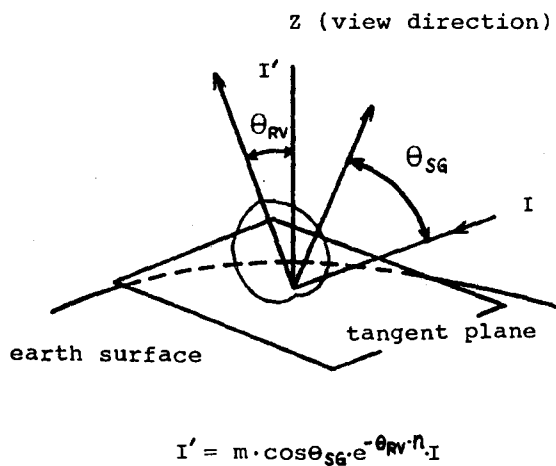
where $N = (\tan^2\theta_x + \tan^2\theta_y + 1)^{1/2}$

and the direction cosines of the sun light axis S_x, S_y, S_z are expressed as

$$\begin{aligned} S_x &= \cos\theta_d \cdot \cos\theta_h \\ S_y &= \sin\theta_d \cdot \cos\theta_h \\ S_z &= \sin\theta_h \end{aligned} \dots (5)$$

The angle between the normal of the earth surface and sun light axis is now expressed as

$$\cos\theta_{sg} = S_x G_x + S_y G_y + S_z G_z \dots (6)$$



$$I' = m \cdot \cos\theta_{sg} \cdot e^{-\theta_{rv} \cdot n} \cdot I$$

Fig.8 The three dimensional model of light reflectance .

On the other hand, the direction cosines of the reflected light axis by the earth surface R_x, R_y, R_z are

$$\begin{aligned} R_x &= S_x - 2G_x * \cos\theta_{sg} \\ R_y &= S_y - 2G_y * \cos\theta_{sg} \\ -R_z &= S_z - 2G_z * \cos\theta_{sg} \end{aligned} \quad \dots\dots(7)$$

Cosine of the angle between the reflected light axis and the zenith, θ_{rv} , can be expressed as

$$\begin{aligned} \cos\theta_{rv} &= R_x^2 + R_y^2 + R_z^2 \\ &= R_z \end{aligned} \quad \dots\dots(8)$$

therefore,

$$\theta_{rv} = \tan^{-1}((1-R_z^2)^{1/2} / R_z) \quad \dots\dots(9)$$

By substituting eqs.(6) and (9) to eqs.(3), I' can be acquired.

In eqs.(3), " mI " corresponds to the shadow free LANDSAT image. The parameter " n " decides the reflection characteristics of the earth surface. If $n=0$, the earth surface is a perfectly diffused reflector and if $n=\infty$, it is a specular reflector.

In this research, n was decided interactively. Under the same sun elevation and azimuthal angle condition as the original data, n value was decided as to make much the same image as the original image. The decided n value was 0.3.

V. RESULTS AND DISCUSSION

Fig.8 shows the generated virtual LANDSAT MSS images with four sun azimuthal angles. These images show the fact that the impression of the images completely changes according to the sun direction. These image sets will be very effective for human interpretation of the lineaments.

Fig.9 shows the influence of a sun elevation. Large scale structures are very evident in the low angle image, while fine structures appear in the high angle images.

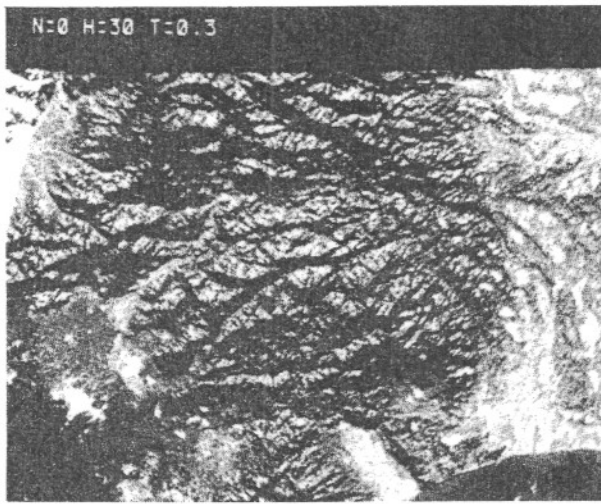
Fig.10 and 11 shows lineament enhanced images from the original image and the virtual image with a perpendicular sun azimuth with the original image, respectively. It is evident that most of the lineaments in Fig.10 run from north east to south west and those in Fig.11 run from north west to south east. Fig.12 shows the composite of Fig.10 and 11 and shows a complete lineaments detection.

AUTHOR BIOGRAPHICAL DATA

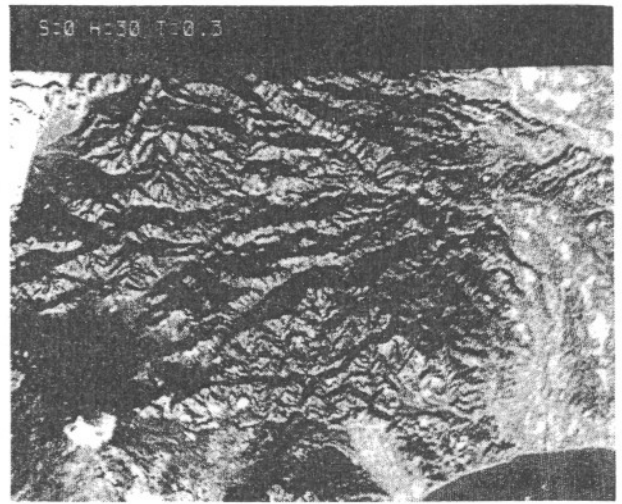
Mr. Kiyonari Fukue received the B.S. and M.S. degrees from the Tokai University of Kanagawa, Japan, in 1976 and 1978, respectively. From April 1978 to March 1981 he was a graduate student of doctor course in the Department of Electro Photo-Optics Engineering, Tokai University. Currently, he is an assistant at the Institute of Research and Development, Tokai University. His research interests include digital image processing and system, especially in remote sensing.

Dr. Haruhisa Shimoda received the Ph.D. degree in solid state physics of Organic semiconductor from the University of Tokyo, Tokyo, Japan, in 1972. Since 1972, he has been an Assistant Professor of the Department of Electro Photo-Optics Engineering at the Tokai University, Kanagawa, Japan. He is currently engaged in field of digital image processing, a development of image processing system, and application of digital image processing to remote sensing.

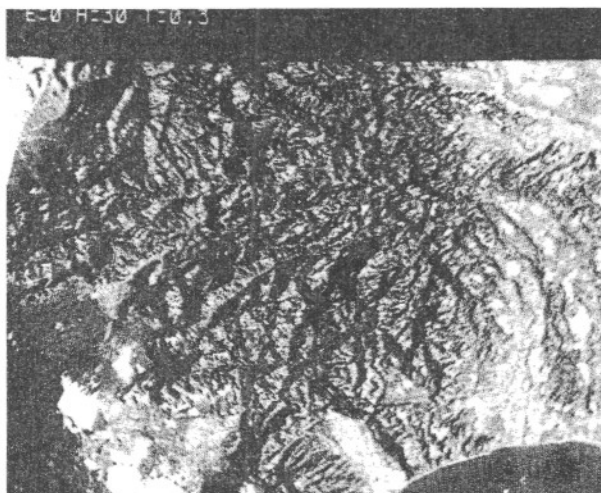
Dr. Toshibumi Sakata received B.S. degree of Chemical Engineering from Chiba University. He took doctor in Engineering of Chemical Physics at the University of Tokyo and then joined to the Institute of Industrial Science there, as a research associate. He was a research scientist of Munich University during 1964 to 1966. In 1966 he moved to the Tokai University and he had a chair of professor in 1971. Presently he is the director of Tokai Research and Information Center, the Tokai University.



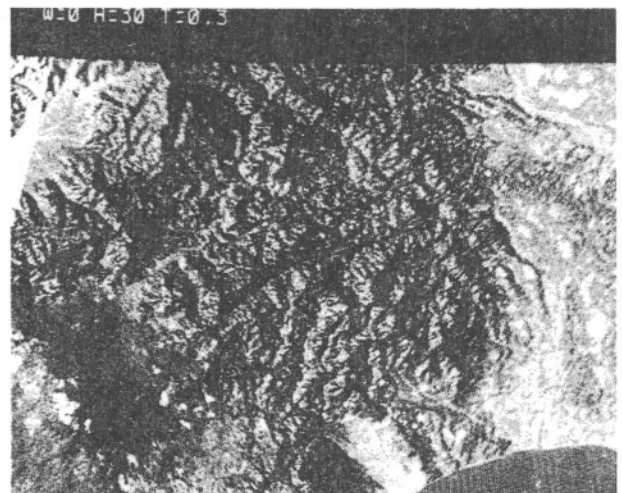
(1)



(2)

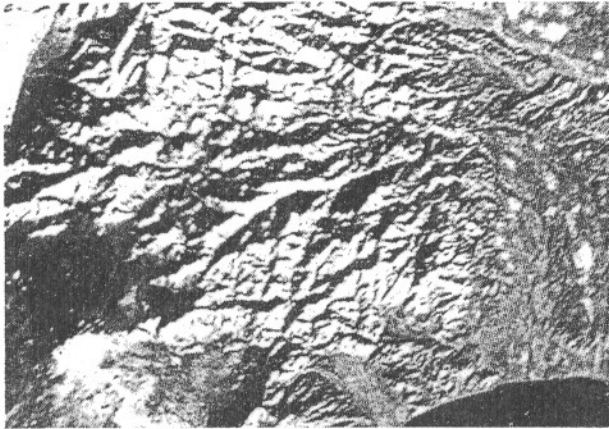


(3)

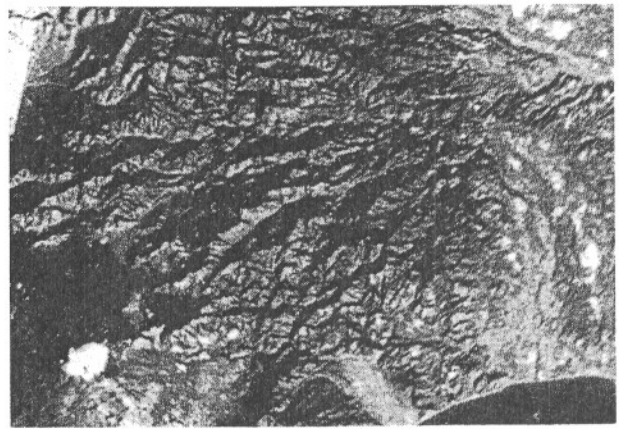


(4)

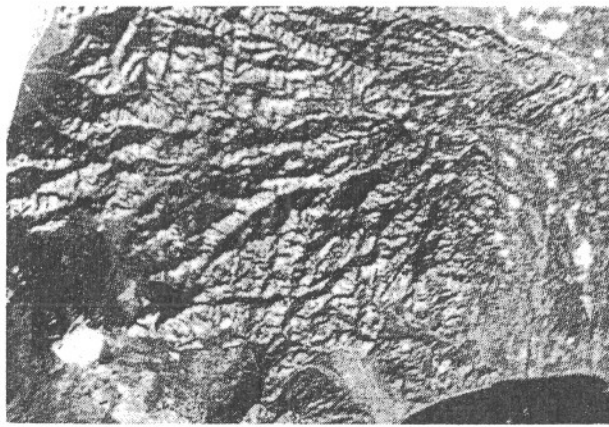
Fig.9 The influence of sun azimuth angle.
(1)north, (2)south, (3)east, and (4)west



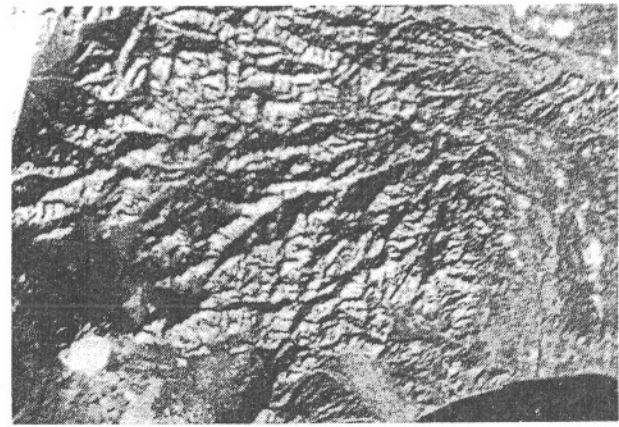
(1)



(2)



(3)



(4)

Fig.10 The influence of sun elevation.
(1)20 , (2)30 , (3)40 , and (4)50

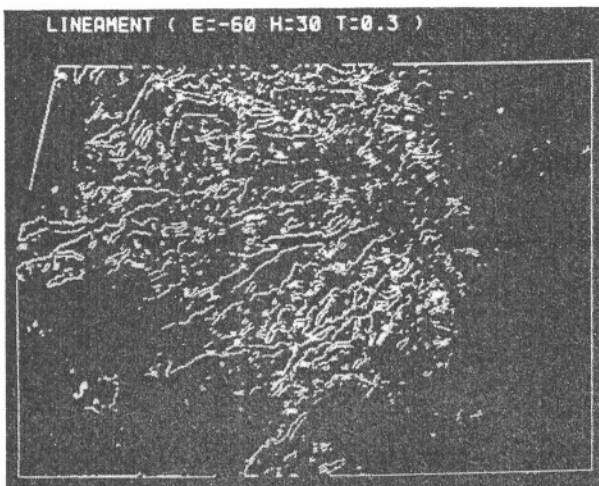


Fig.11 A lineament enhanced image the original image.

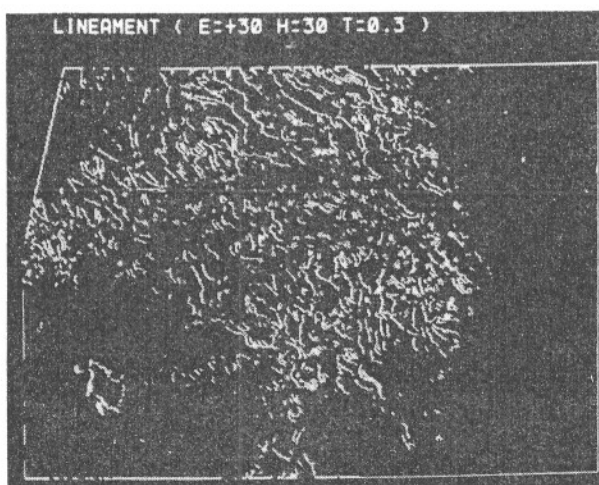


Fig.12 A lineament enhanced image from the virtual image with the perpendicular sun azimuth with the original image.

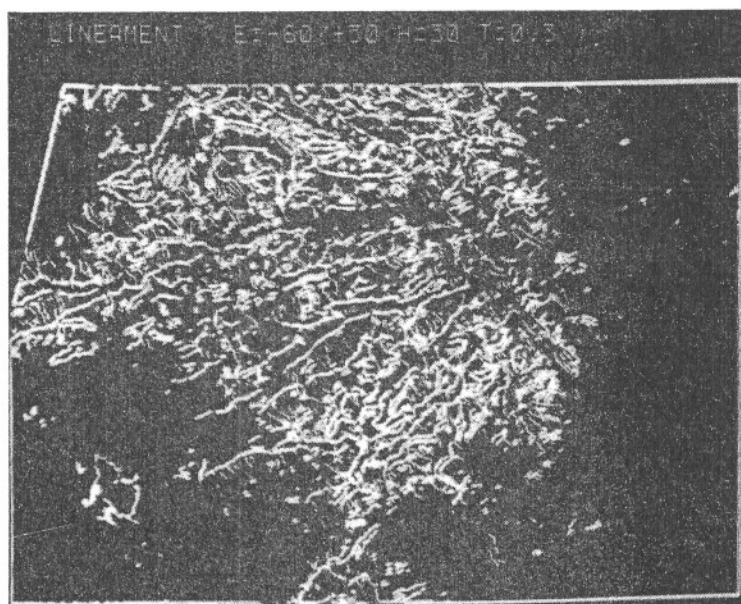


Fig.13 The composed of Fig.10 and Fig.11.